Atmospheric Environment 323 (2024) 120398

Contents lists available at ScienceDirect

Atmospheric Environment

journal homepage: www.elsevier.com/locate/atmosenv

# Assessment and characteristics of S-NPP VIIRS Deep Blue and Dark Target aerosol properties under clean, polluted and fire scenarios over the Amazon

Vanúcia Schumacher [*], Alberto Setzer [1]

*National Institute for Space Research -INPE, General Coordination of Earth Sciences - CGCT, São José dos Campos, SP, Brazil*

## HIGHLIGHTS

- The VIIRS DB product outperforms the DT overall for different aerosol properties.
- Both algorithms indicate poor accuracy in forest coverage.
- VIIRS DT was more sensitive to variation air pollution scenarios.

## ARTICLE INFO

*Keywords:*
Aerosol optical depth (AOD)
Uncertainty evaluation
AERONET
VIIRS
Amazon basin

## ABSTRACT

The present study carries out the systematic performance evaluation of aerosol optical depth (AOD) products retrieved using Visible Infrared Imaging Radiometer Suite (VIIRS) Deep Blue (DB) and Dark Target (DT) onboard Suomi National Polar-orbiting Partnership (S-NPP) satellite over the Amazon Basin. Characteristics and uncertainty were evaluated under distinct air pollution scenarios such as a clean background in the wet season, polluted conditions in the dry season with biomass burning emissions and peak burning season with higher fire activity. VIIRS retrievals were also analyzed under aerosol loading, particle size and surface vegetation coverage against the Aerosol Robotic Network (AERONET) measurements at 9 sites in 2012–2022. VIIRS DB showed good accuracy, with 78% of AOD matchups falling within the expected error, 84% in the wet season, and 71% in the dry and burning seasons. In contrast, VIIRS DT indicated poor accuracy (64%) and trends overestimate the AOD in all air pollution scenarios. Both algorithms were sensitive to AERONET sites with high elevation and dark vegetated coverage characteristics. VIIRS DB and DT systematically overestimated AERONET AOD as increased aerosol loading. DB trends underestimate aerosol under background conditions and overestimate with coarse and fine particle predominance. Additionally, both algorithms indicated poor accuracy under forest type with a large positive bias. VIIRS DB demonstrated the highest accuracy in the presence of aerosol loading in sites characterized by mixed land cover type. This was observed in both coarse and fine mode scenarios for grassland. VIIRS DT demonstrated satisfactory accuracy under background conditions and dominance of coarse particles within grassland land cover type. For mixed land cover, satisfactory accuracy was found under intermediate aerosol loading conditions. DB algorithm showed greater uncertainty associated with the coarse particle aerosol for the full period and all polluted scenarios. Overall, VIIRS DT accuracy was more sensitive to varying air pollution scenarios.

## 1. Introduction

Atmospheric aerosols emitted from natural and anthropogenic sources play a crucial role in modulating climate through scattering and absorbing sunlight, affecting the atmospheric radiation balance (Bellouin et al., 2020; Kok et al., 2023). The complex aerosol-cloud-radiation interactions can lead to net radiative cooling or heating on global and regional scales, where the radiative forcing estimation represents one of the largest uncertainties in climate change predictions (IPCC, 2021; Ren-Jian et al., 2012). Besides climate effects, high aerosol concentration also implies several impacts on human health risks and diseases (Butt et al., 2016; Mushtaq et al., 2022).

* Corresponding author.
*E-mail address:* vanucia-schumacher@hotmail.com (V. Schumacher).
[1] deceased: 08/09/2023.

https://doi.org/10.1016/j.atmosenv.2024.120398
Received 25 September 2023; Received in revised form 18 January 2024; Accepted 11 February 2024
Available online 12 February 2024

To understand the diverse effects of aerosols, Aerosol Optical Depth (AOD) is commonly used to describe aerosol loadings and properties, mainly associated with air quality concerns (e.g., Wang et al., 2023). The AErosol RObotic NETwork (AERONET) provides observations of spectral AOD based on calibrated ground-based Sun photometers with high temporal resolution distributed globally (Holben et al., 1998); however, they are constrained to specific locations, have sparse spatial coverage, and may present data gaps. Remote sensing using accurate long-term aerosol satellite-based datasets with global spatial coverage, including in areas where ground-based data are unavailable, is essential to overcome these limitations (Aditi et al., 2023; Su et al., 2023; Wei et al., 2019b).

Several studies have been carried out on global and regional scales, over land and ocean, focused on validating and comparing satellite-based datasets and ground-observed aerosol data, mostly based on satellite instruments such as Moderate Resolution Imaging Spectroradiometer (MODIS) Dark Target (DT) and Deep Blue (DB) AOD products (Chu et al., 2002; Huang et al., 2023; Sayer et al., 2013; Wei et al., 2019a), MODIS Multi-Angle Implementation of Atmospheric Correction (MAIAC) (Falah et al., 2021; Qin et al., 2021; Rogozovsky et al., 2023; Wang et al., 2022), Multi-angle Imaging Spectro-Radiometer (MISR) (Fan et al., 2023; Gui et al., 2021; Martonchik et al., 2004), and Visible Infrared Imaging Radiometer Suite (VIIRS) (Aditi et al., 2023; Payra et al., 2023; Su et al., 2022, 2023; Wang et al., 2023). These results improved AOD algorithms and retrieval uncertainty under distinct aerosol properties and characteristics.

VIIRS is a new generation satellite sensor onboard the Suomi National Polar-orbiting Partnership (S-NPP) launched in late 2011 as a successor to MODIS for Earth data products generation; VIIRS AOD products from the Collection 6 of MODIS data (Hsu et al., 2019) have shown excellent performance globally, with about 80% of retrievals falling within the expected error level (Hsu et al., 2019; Sayer et al., 2019; Su et al., 2023; Wang et al., 2023). Additionally, the VIIRS DB AOD algorithm is more accurate than the DT AOD product on global and regional scales (e.g., He et al., 2021; Su et al., 2021; Wang et al., 2020; Wang et al., 2023). Su et al. (2023) evaluated different AOD products over land and ocean and showed better performance of the VIIRS DB algorithm compared to MODIS DB, DT, MAIAC, VIIRS DT and NOAA products. VIIRS DB presented high accuracy in the ocean and land, and best validation metrics on regional and site-by-site comparison, including over the Central/South America. On the contrary, Aditi et al. (2023) showed unsatisfactory retrieval accuracy by both VIIRS DB and DT over South Asia, while Su et al. (2022) reported that VIIRS DB presented the highest accuracy in Asia.

Although several studies have evaluated and compared current satellite-based AOD products, the accuracy of VIIRS DB and DT AOD retrievals has not been extensively investigated on the regional scale, with few studies centered mostly in China and Asia. Previous studies focused on global performance also indicate site-scale evaluations account for South America (e.g., Gumber et al., 2022; Su et al.; Wang et al., 2023) or consider just one AERONET site in the entire Amazon (e.g., Chen et al., 2022; Hsu et al., 2019), which can lead to inconsistencies about the performance and applicability of the AOD algorithms in this complex region.

The Amazon Basin, with ~7 million km$^2$ and spanning nine countries in South America, is characterized by diverse climate range, relief, land cover and land use types (Davidson et al., 2012; Lima et al., 2012; Montalván-Burbano et al., 2021; Pires, 1984). It contains ~40% of the world's tropical rainforests, with ~5.5 million km$^2$ in nine countries, of which ~60% are in Brazil. The basin also encompasses extensive grasslands and vast deforested areas dedicated to agriculture and cattle ranching, where fires of anthropic origin occur periodically (Eufemia et al., 2022; Lapola et al., 2023). The Amazon Basin's ecosystem is highly vulnerable to climate change impacts, mostly related to alterations in the water cycle and land use changes associated with extensive fires and deforestation (Arias et al., 2020; Llopart et al., 2018). Additionally, deforestation over the Amazon basin increases by up to 57% the frequency of longer dry seasons in the central-southern Amazon (Ruiz-Vásquez et al., 2020).

The intense fire activity in the Amazon also harms human health (Ignotti et al., 2010; Morello, 2023). Rocha and Sant'Anna (2022) showed that exposure to air pollution increases hospitalizations for respiratory diseases in the Brazilian Amazon by up to 14% when levels of fine particulate matter reach three times the threshold recommended by the World Health Organization (WHO). New deforestation should lead to a tipping point in the Amazon climate, aggravated by the use of fire in new clearings and as a common practice in agriculture and ranching, with negative impacts on different subjects, such as biodiversity, Indigenous populations, freshwater supply, rainfall variability, climate patterns, air quality regulation, and carbon sequestration to mitigate climate change (Lovejoy and Nobre, 2019; Prist et al., 2023; Xu et al., 2022).

Due to its regional diversity, data from a single AERONET site may only partially capture the complexity and heterogeneity of aerosol distributions across the entire Amazon. Therefore, a comprehensive VIIRS AOD evaluation with multiple AERONET sites is crucial to understanding the performance under polluted and clean backgrounds in this complex environment.

This study provides an evaluation and comparison of the VIIRS DB and DT AOD retrieval algorithm against AERONET measurements in the Amazon Basin. Retrieval uncertainty and characteristics under distinct air pollution scenarios over the last 11 years (from 2012 to 2022) were analyzed under varying aerosol magnitude loading, particle size distribution and surface vegetation coverage. As the first VIIRS systematic analysis in the Amazon, known for its complex air pollution levels with high rates of fires and deforestation, we expect to highlight valuable insights for VIIRS DB and DT algorithms improvement and application in this critical region.

## 2. Data and methods

### 2.1. AERONET AOD products

AERONET is a global ground-based network of calibrated sun photometers and sky radiometers that provide quality-assured aerosol properties every 15 min in several spectral channels between 0.340 and 1.640 μm (Holben et al., 1998). Aerosol optical properties are available in three categories: level 1.0 (unscreened), level 1.5 (cloud screened), and level 2.0 (cloud screened and high quality assured), available at https://aeronet.gsfc.nasa.gov/. This study used Version 3 level 2.0 with high-quality-controlled AOD and Angstrom Exponent (AE) products (Giles et al., 2019) and spectral deconvolution algorithm (SDA) to derive coarse and fine mode from spectral AOD of the direct sun measurements (O'Neill et al., 2001; 2003, 2006). To ensure consistent records, we eliminated AERONET sites with less than one year and selected sites with at least 25 matchups, obtaining nine stations from 2012 to 2022 for evaluation in the Amazon Basin. The study period was selected based on satellite data availability. Fig. 1 shows the spatial distribution of the selected AERONET sites, while Table 1 summarizes the AOD retrieved information.

### 2.2. VIIRS DB and DT AOD products

The VIIRS provides satellite-derived measurements of AOD and their properties for bright surfaces and vegetated and dark surfaces based on MODIS DB and DT algorithms, with daily global coverage (Hsu et al., 2019; Sawyer et al., 2020). We used Level-2 (L2) Deep Blue aerosol product (AERDB_L2_VIIRS_ SNPP) and Dark Target aerosol product (AERDT_L2_VIIRS_SNPP), Version 2.0 (V2.0) with the best-estimate Quality Assurance (QA) filtered at 550 nm, named "Aerosol_Optical_Thickness_550_Land_Best_Estimate" and "Optical_Depth_Land_And_Ocean", respectively; with a spatial resolution of 6

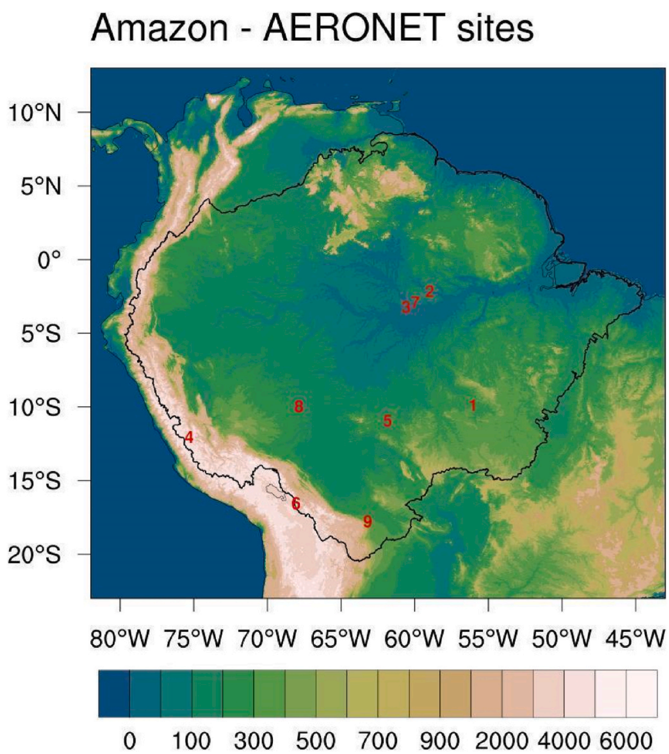


**Fig. 1.** Location of the Amazon Basin in South America with the nine AERONET sites indicated by the numbers in red and the mean topography according to the color scale in meters.

km × 6 km from 2012 to 2022 because the VIIRS product is available starting on March 2012. V2.0 VIIRS DB has some improvements concerning Version 1.1, such as QA filtering, smoke detection scheme, and retrieval accuracy for fine-mode dominant aerosol. VIIRS DB and DT AOD products are downloaded from NASA's Level-1 and Atmosphere Archive and Distribution System (LAADS) Distributed Active Archive Center (DAAC) at https://ladsweb.modaps.eosdis.nasa.gov/.

### *2.3. Spatiotemporal colocation and evaluation metrics*

To compare and validate VIIRS DB and DT AOD retrievals against point-based AERONET AOD measurements, we applied a spatio-temporal matchup scheme as discussed by Ichoku et al. (2002) and Petrenko et al. (2012). A spatial window of the 27.5 km circle radius centered at each AERONET site was used for VIIRS DB and DT AOD retrieval while a temporal 1-h window (±30 min of VIIRS overpass) was used to average AERONET AOD measurements. Only the best and quality-assured VIIRS DB (QA = 2 and 3) and DT (QA = 3) AOD retrievals were considered in this analysis.

The AERONET has no AOD values at 550 nm as VIIRS DB and DT. For direct comparison, AERONET AOD was interpolated into 550 nm based on the Angstrom Exponent (440–675 nm) (Eck et al., 1999; Falah et al., 2021). AERONET SDA data was also converted to 550 nm using the fine mode and total AOD, and the corresponding AE within the SDA product; then, AOD coarse mode at 550 nm was computed simply as the difference of total AOD and fine mode (e.g.; Peng et al., 2023).

The air pollution scenarios were defined as a clean background in the wet seasons (February to May), a polluted condition in the dry seasons with biomass burning emissions (August to November), and a peak burning season that corresponds to a critical period with the highest occurrence of fires in the Amazon Basin (September) (e.g., Palácios et al., 2022).

Additionally, the Sentinel-2 based ESRI Land Cover with 10m spatial resolution (Karra et al., 2021) is used to select the Land Cover characteristics related to the spatial window around each AERONET site. The original ESRI class names were reclassified into generic land cover names (Table 2). We considered the major Land Cover type with at least 50% within the AERONET spatial window, while AERONET sites with less than 50% of a predominant Land Cover type were defined as mixed type (Table 2). Then, three major Land Cover types were derived in the Amazon Basin: Grassland, Forest and Mixed types (Fig. 2).

Several statistics were used: Pearson correlation coefficient (R), coefficient of determination ($R^2$, Eq. (1)), relative mean bias (RMB, Eq. (2)), root-mean-square error (RMSE, Eq. (3)), and Expected Error (EE, Eq. (4)). RMB values greater than 1 indicate the average overestimation, whereas RMB values less than 1 indicate the average underestimation of AOD retrievals. EE is commonly used to evaluate satellite retrieval uncertainties and is considered satisfactory accuracy when more than 66% of the difference between VIIRS AOD algorithms and AERONET AOD falls within the EE envelope (Levy et al., 2015). N is the number of collocated points. The equations for comparing satellite AOD products and AERONET are described below:

$$R^2 = 1 - \frac{\sum_{i=1}^{n}\left(AOD_{(SATELLITE)i} - AOD_{(AERONET)i}\right)2}{\sum_{i=1}^{n}\left(AOD_{(SATELLITE)i} - \overline{AOD}_{(SATELLITE)}\right)2} \tag{1}$$

$$RMB = \frac{\overline{AOD}_{SATELLITE}}{\overline{AOD}_{AERONET}} \tag{2}$$

$$RMSE = \sqrt{\frac{1}{N}\sum_{i=1}^{n}\left(AOD_{(SATELLITE)i} - AOD_{(AERONET)i}\right)2} \tag{3}$$

$$EE = \pm\left(0.05 + 0.15AOD_{AERONET}\right) \tag{4}$$

**Table 1**
Aeronet sites in the Amazon region were used in this study. The ID number is a reference to the site location in Fig. 1.

| ID | Aeronet sites | Lat | Lon | Elev | LC type | Year | $N_{available}$ | $N_{DB}$ | $N_{DT}$ |
|---|---|---|---|---|---|---|---|---|---|
| 01 | Alta Floresta | 9.871S | 56.104W | 277 | Mixed | 2012–2021 | 30318 | 515 | 573 |
| 02 | Amazon ATTO Tower | 2.144S | 59.000W | 210 | Forest | 2016–2021 | 22543 | 45 | 183 |
| 03 | ARM Manacapuru | 3.213S | 60.598W | 50 | Forest | 2013–2015 | 4348 | 25 | 103 |
| 04 | Huancayo-IGP[a] | 12.040S | 75.321W | 3313 | Grassland | 2015–2022 | 133324 | 524 | 551 |
| 05 | Ji_Parana_SE | 10.934S | 61.852W | 218 | Grassland | 2012–2021 | 32813 | 428 | 547 |
| 06 | La Paz[b] | 16.539S | 68.066W | 3439 | Grassland | 2012–2022 | 78226 | 851 | 838 |
| 07 | Manaus Embrapa | 2.891S | 59.970W | 115 | Forest | 2012–2019 | 13729 | 30 | 184 |
| 08 | Rio Branco | 9.957S | 67.869W | 212 | Grassland | 2012–2021 | 31054 | 277 | 366 |
| 09 | Santa Cruz Utepsa | 17.767S | 63.201W | 432 | Mixed | 2012–2022 | 45428 | 602 | 625 |

[a] Peru.
[b] Bolívia. Brazil, for all the others. $N_{available}$ is the number of daily average data, $N_{DB}$ and $N_{DT}$ are the numbers of daily matchup data with respect to VIIRS DB and DT, respectively, Elev is the elevation in meters, and LC type is the major land cover type.

**Table 2**
The Land Cover types around each AERONET site. Mixed type (M) is defined by AERONET sites with less than 50% of one predominate Land Cover type. Adapted from ESRI Land Cover.

| Code of Class | Original Class | Name adopted | ID AERONET sites | | | | | | | | |
|---|---|---|---|---|---|---|---|---|---|---|---|
| | | | 1 | 2 | 3 | 4 | 5 | 6 | 7 | 8 | 9 |
| 1 | Water | Water (W) | 1% | 6% | 27% | 0.4% | 1% | 0.4% | 0.1% | 1% | 0.4% |
| 2 | Trees | Forest (F) | 38% | 93% | 50% | 2% | 24% | 0.3% | 98% | 39% | 46% |
| 4 | Flooded Vegetation | Flooded (FV) | 0% | 1% | 19% | 0% | 0% | 0% | 0% | 0.4% | 0% |
| 5 | Crops | Croplands (C) | 16% | 0% | 0.3% | 11% | 1% | 2% | 0% | 3% | 9% |
| 7 | Built Area | Urban (U) | 1% | 0.1% | 2% | 9% | 2% | 13% | 1% | 5% | 20% |
| 8 | Bare ground | Arid Lands (AL) | 0% | 0% | 0.1% | 0.2% | 0% | 9% | 0% | 0% | 1% |
| 9 | Snow/ice | Snow/ice (SI) | 0% | 0% | 0% | 0% | 0% | 0.4% | 0% | 0% | 0% |
| 10 | Clouds | Clouds (CL) | 0% | 0% | 0% | 0% | 0% | 0% | 0% | 0% | 0% |
| 11 | Rangeland | Grassland (G) | 44% | 0.2% | 2% | 78% | 72% | 75% | 1% | 52% | 25% |
| | Major Land Cover | | M | F | F | G | G | G | F | G | M |

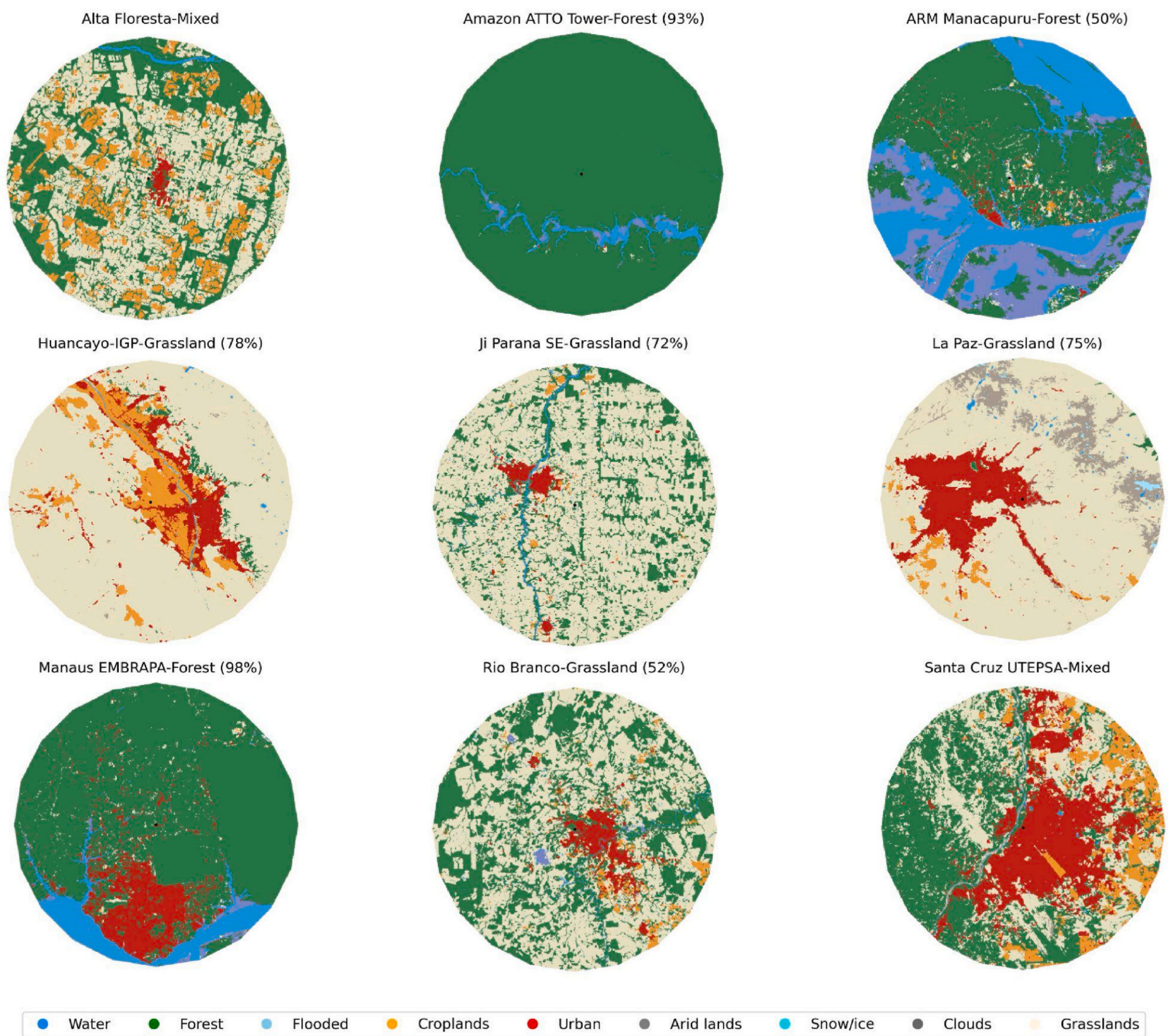


**Fig. 2.** The land cover types around spatial windows centered at each AERONET site from ESRI Land Cover data. The name and the number on the top represent the AERONET site with respectively major land cover type and area percentages.

## 3. Results and discussion

### *3.1. Overall accuracy evaluation and comparison*

The accuracy retrieval of VIIRS-AERONET matchups in the Amazon is shown in Fig. 3. The overall performance indicates high accuracy for VIIRS DB with 78% retrieval, thus falling within the one-standard-deviation confidence interval of AERONET AOD, with a high correlation of 0.93 ($R^2 = 0.86$) and an RMB close to the non-bias value of 1. Unsatisfactory retrieval accuracy is recorded for VIIRS DT with 64% within EE, although with good agreement with AERONET by correlation of 0.91 ($R^2 = 0.78$) and RMB of 1.13. These findings are consistent with VIIRS DB performance in Asia with an EE of 77% and R of 0.91 (Su et al., 2022), although less accurate than VIIRS DB on global land assessments (EE = 83%; Wang et al., 2023). Similar results with VIIRS DB outperforming VIIRS DT AOD are also reported globally and in East China

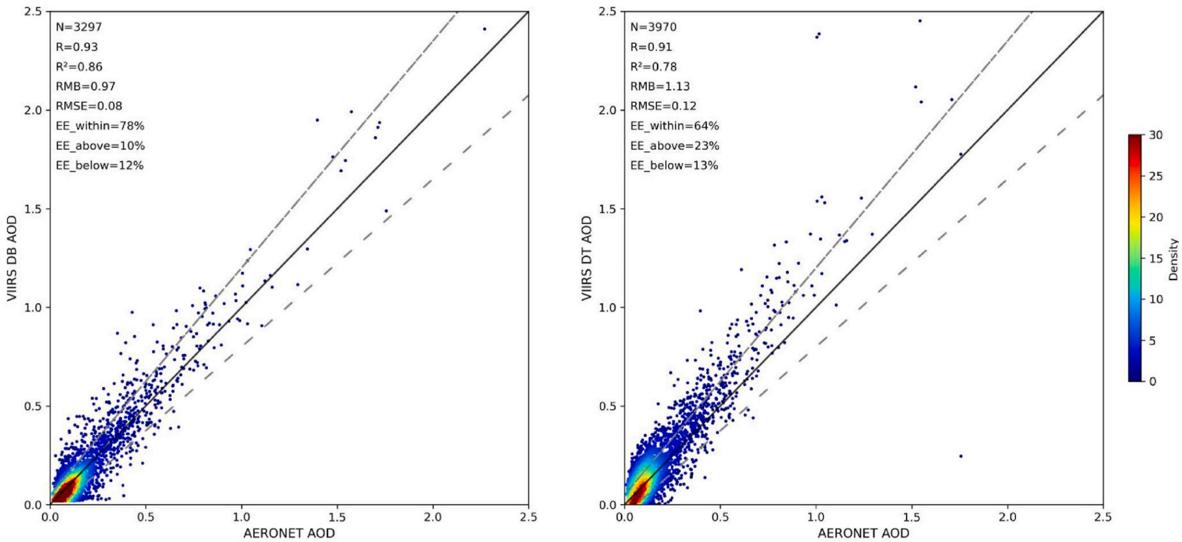


**Fig. 3.** Evaluation of VIIRS DB and VIIRS DT AOD 550 nm product retrievals against AERONET AOD measurements for all sites over the Amazon Basin. The dashed lines refer to the expected error envelope (EE = $\pm(0.05 + 0.15 \times \text{AOD}_{\text{AERONET}})$ and the black solid line is the 1:1 line. The colors show the density of the data points. Performance metrics are shown in the upper left corner of each panel. N is the total number of matched AOD data points.

(Su et al., 2021; Wang et al., 2023).

The seasonal performance (Fig. 4) shows higher accuracy for VIIRS DB in the wet season with 84% within the confidence interval, although with a low correlation but significant statistically (R = 0.47; $R^2$ = 0.20) and a lower number of matchups (N = 565) compared to the dry season. It is expected that during the wet season, more cloud-related gaps occur in VIIRS AOD retrievals and AERONET measurements (e.g., Hsu et al., 2019). VIIRS DB also indicates high accuracy in the dry season and during the peak burning season, both with 71% within EE and a correlation of 0.93 and 0.94, respectively. Conversely, VIIRS DT presents unsatisfactory accuracy in terms of retrievals falling within the EE, with 63%, 61% and 64% in the wet-dry-burning seasons, although it shows similar correlations compared to VIIRS DB algorithm, 0.35, 0.93 and 0.94, respectively.

Overall, VIIRS DB slightly underestimates AOD compared to AERONET (RMB = 0.97), except in the wet season (RMB = 1.11) while widespread overestimates are shown for VIIRS DT (RMB = 1.13), being more pronounced also in the wet season (RMB = 1.37) (Figs. 3 and 4). Clearly, a systematic negative (positive) bias can be noted in almost all years to VIIRS DB (DT), except for the wet season (Fig. 5c and d). VIIRS DB indicates lower biases than VIIRS DT for almost all years, with large bias values occurring for both algorithms in the wet and dry seasons.

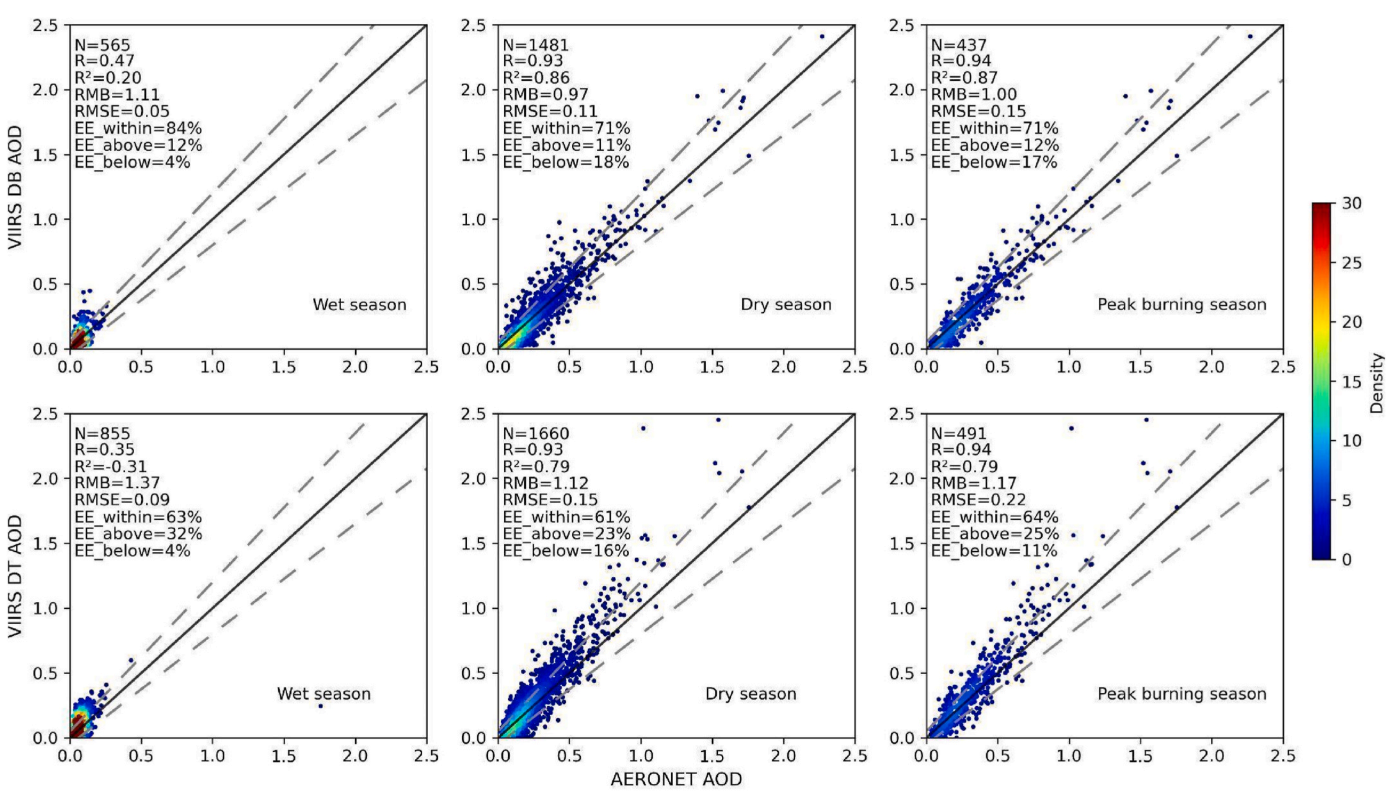


**Fig. 4.** Same as Fig. 3 but for seasonal variations of retrieval accuracy of VIIRS DB and DT AOD against AERONET AOD over the Amazon Basin.

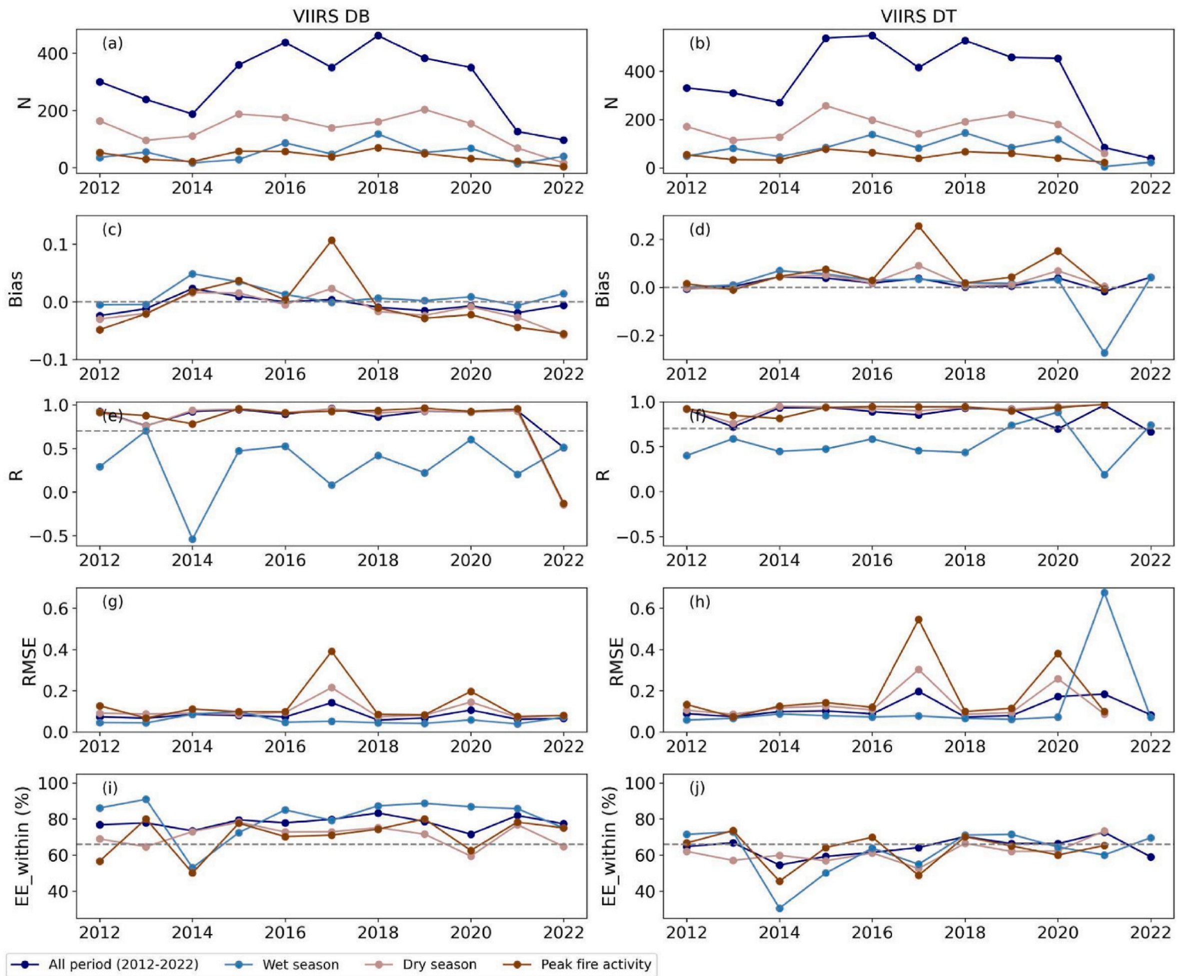


**Fig. 5.** Time series of (a–b) number of matchups, (c–d) bias between VIIRS DB and DT AOD and AERONET AOD, (e–f) R, (g–h) RMSE, and (i–j) within EE over the Amazon Basin.

Higher positive bias is shown in 2014 in both algorithms in the wet season with low correlation, unsatisfactory retrieval within EE and a lower number of matchups, especially for DB. A pronounced negative bias in the wet season in 2021 also occurs in VIIRS DT with low correlations, high RMSE and lower accuracy and matchups. Besides these biases, higher RMSE is also associated with a large positive bias in the dry season for both algorithms, probably caused by high aerosol events.

VIIRS DB and DT retrievals show good agreement with AERONET measurements considering the 2012–2022 period and in the dry season, with high correlations ($R > 0.7$) in almost all years (Fig. 5e and f). A poor agreement with $R < 0.7$ is noted in the wet and peak burning seasons, probably associated with fewer matchups in these air pollution scenarios. In terms of RMSE, both VIIRS DB and DT show the same pattern over the years, whereas VIIRS DT has slightly higher values than VIIRS DB, mainly in the year 2021, considering the full period and in the wet season (Fig. 5g and h). On the other hand, VIIRS DB outperforms VIIRS DT in almost all years in terms of EE envelope, with the best accuracy considering all period and in the peak burning season. VIIRS DT also presents the best accuracy in the burning season, with almost all years achieving at least 66% of matchups falling within the EE range (Levy et al., 2015) (Fig. 5g and h).

### *3.2. Site-scale evaluation*

The performance of VIIRS DB and DT AOD retrievals for each site in the Amazon Basin is shown in Fig. 6. In general, VIIRS DB AOD shows a good agreement with AERONET measurements, with six AERONET sites (Alta Foresta, Huancayo-IGP, Ji Parana SE, La Paz, Rio Branco and Santa Cruz Utepsa) having between 68 and 91% matchups within the EE envelopes. Conversely, VIIRS DT is consistent with AERONET AOD only over four sites (Huancayo-IGP, La Paz, Rio Branco and Santa Cruz Utepsa). However, although the Huancayo-IGP and La Paz sites have 91% and 72% (66% and 81%) within the EE in DB (DT), respectively, very low correlation and significative negative deviations suggest poor performance and a strong underestimate. These sites in the Peruvian and Bolivian Amazon have higher elevations (>3000 m altitude, see Table 1), located in the Andean region surrounded by mountainous terrain (see Fig. 1) which can lead to limitations on AOD retrieval. Wang et al. (2023) also reported poor performance of VIIRS AOD retrievals over mountain regions. Chen et al. (2022) evaluated MODIS, MISR and VIIRS and showed a low correlation over AERONET sites located around elevated terrain (Sierra Nevada), Andes Mountains and coastal regions.

It is interesting to note that both Huancayo-IGP and La Paz sites exhibit very similar spatial characteristics of the grassland land cover type (Fig. 2). This is in contrast to Ji Parana SE and Rio Branco sites, which, despite also having grassland features, present more stratified terrain that includes forests. The land cover type characteristics could affect the reflected sunlight, impacting the albedo retrieval and leading to the surface bidirectional reflectance distribution function (BRDF) effect. Peng et al. (2023) evaluated NOAA and VIIRS surface albedo characteristics and showed an increased uncertainty related to sites with terrain effects associated with the BRDF, which is modified by the microarea topography. They also pointed out that the BRDF showed nearly isotropic reflectance over bright surfaces.

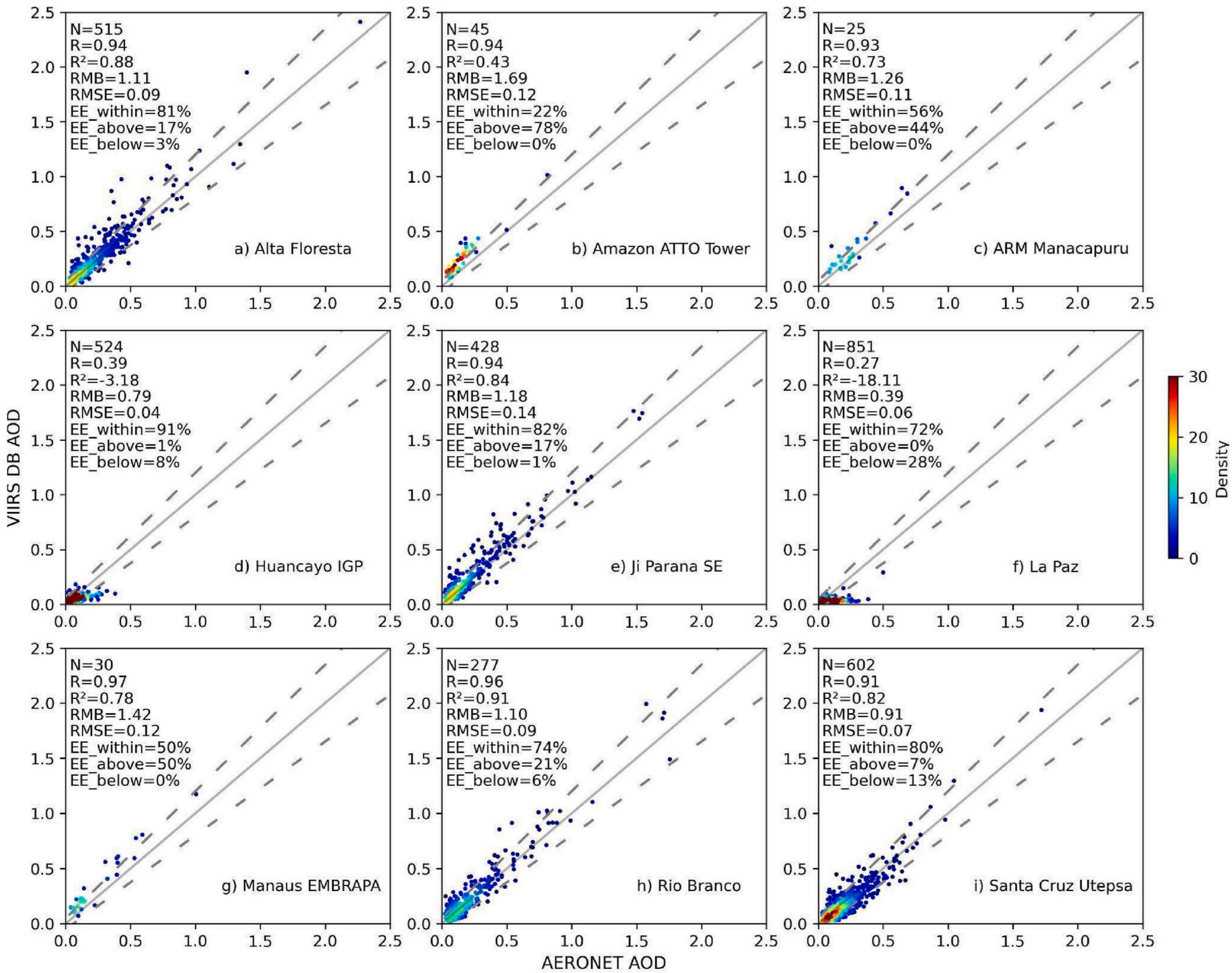


**Fig. 6.** Same as Fig. 3 but for VIIRS DB AOD for each AERONET site.

VIIRS DB (DT) shows the best accuracy over Alta Floresta, Ji Parana SE, Rio Branco and Santa Cruz Utepsa sites (Rio Branco and Santa Cruz Utepsa) with high matchups within the EE, high correlation, and low RMSE, although with a positive bias, except for Santa Cruz Utepsa with slight underestimation AOD retrievals. In addition, a high correlation >0.91 followed by moderate RMSE <0.17, overall overestimation (RMB>1.26), and lower percentages of matchups within the EE (13–56%) are recorded for both VIIRS DB and DT over the Amazon ATTO Tower, ARM Manacapuru and Manaus Embrapa, all sites surrounded by forest surface coverage. These results suggest higher retrieval uncertainty under densely vegetated surfaces and high elevations in the Amazon. Jiang et al. (2022) also indicated poor performance in VIIRS AOD retrievals for forest land cover type over China linked to DB algorithm limitations that led to the overestimation, with the best performance in cropland type. On the contrary, He et al. (2021) showed good performance of VIIRS DB AOD under forest and mountain land use types over China.

In the wet season (Table 3), high accuracy is achieved at one site (Santa Cruz Utepsa) with 88% and 77% within the EE and a correlation of 0.65 and 0.77 for VIIRS DB and DT, respectively. As shown in Figs. 4 and 5, a widespread overestimation of VIIRS DB and DT AOD retrievals is found in all AERONET sites, except for two sites with higher elevation. Interestingly, VIIRS DT has better retrievals than DB regarding the number of matchups over sites with forest land cover type in the wet season, probably associated with DT algorithm characteristics. The performance of VIIRS DB increases in the dry and burning seasons (Table 3), with four sites (Alta Floresta, Ji Parana SE, Rio Branco and Santa Cruz Utepsa) presenting EE >74%, high correlation >0.91 and a slight positive bias, except at the Santa Cruz Utepsa site, where negative bias prevail. On the other hand, DT shows a good performance in Rio Branco and La Paz in the dry and burning seasons, with the best accuracy in La Paz during the peak burning season, with 84% within EE, 0.77 of correlation, lower RMSE and with a significant negative bias (RMB: 0.78) and a lower number of matchups than VIIRS DB.

### 3.3. Accuracy of VIIRS AOD under aerosol loading and particle size

VIIRS DB and DT AOD retrievals are also assessed according to the magnitude of aerosol loading and particle size, where these properties contribute to significant uncertainty on satellite retrievals of the top of the atmosphere (TOA) reflectance (Falah et al., 2021; Mhawish et al., 2019; Sayer et al., 2014). To evaluate aerosol particle size dependence on VIIRS AOD retrieval, we considered the AERONET SDA product as the ground truth to partition the coarse mode, e.g., dust and fine

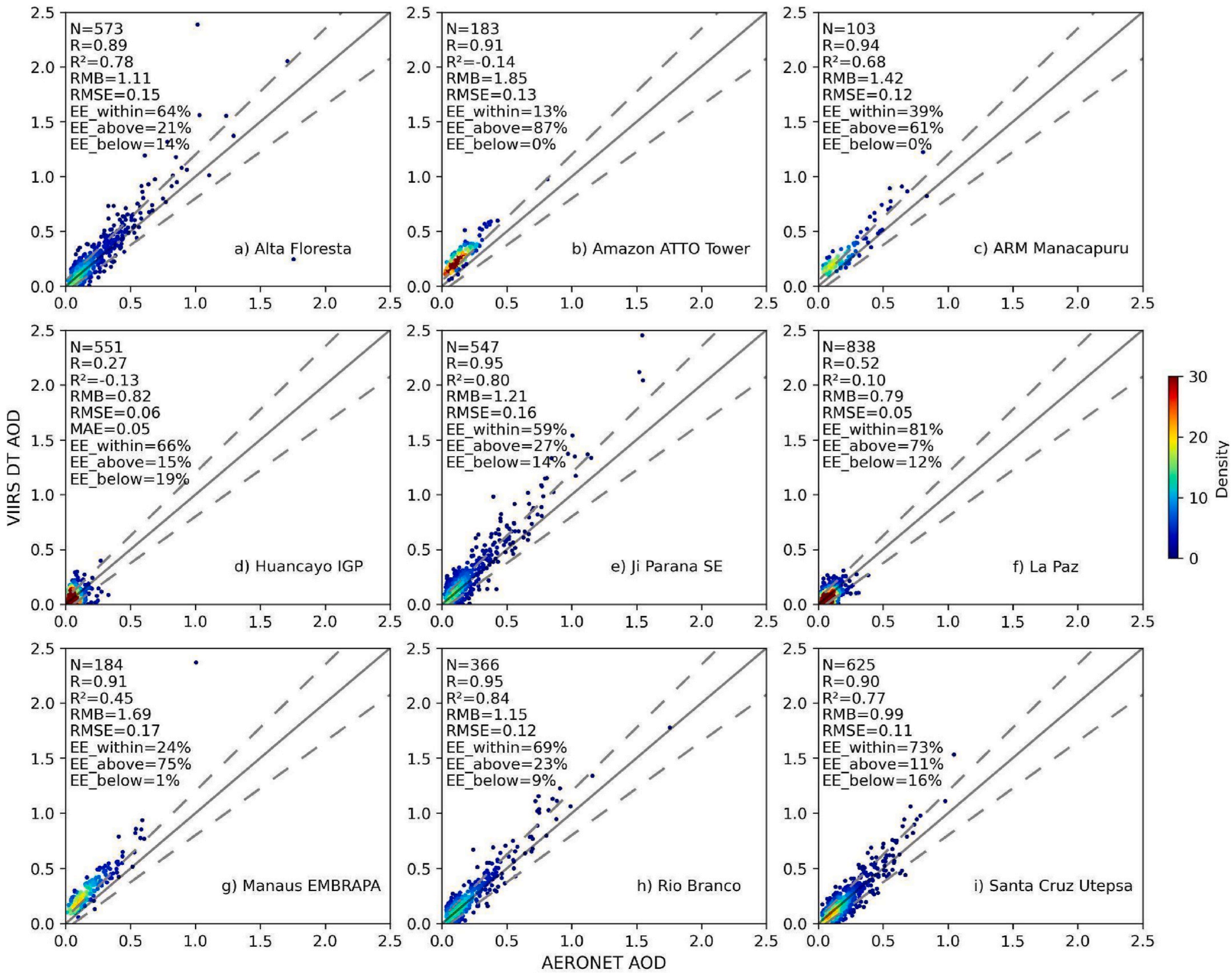


**Fig. 6.** (*continued*).

**Table 3**
Seasonal statistics for the comparison of VIIRS DB and DT AOD retrievals against each AERONET site over the Amazon Basin.

| Algorithm | Aeronet | Wet season | | | | | Dry season | | | | | Peak burning season | | | | |
|---|---|---|---|---|---|---|---|---|---|---|---|---|---|---|---|---|
| | | N | R | RMB | RMSE | EE | N | R | RMB | RMSE | EE | N | R | RMB | RMSE | EE |
| VIIRS DB | Alta Floresta | 52 | 0.29 | 1.76 | 0.08 | 63 | 289 | 0.94 | 1.08 | 0.11 | 78 | 90 | 0.95 | 1.03 | 0.14 | 77 |
| | Amazon ATTO Tower | 5 | 0.75 | 2.05 | 0.08 | 40 | 20 | 0.94 | 1.54 | 0.14 | 25 | 4 | 1.00 | 1.35 | 0.13 | 25 |
| | ARM Manacapuru | 2 | – | – | – | – | 19 | 0.96 | 1.21 | 0.10 | 58 | 6 | 0.74 | 1.16 | 0.08 | 50 |
| | Huancayo-IGP | 108 | 0.19 | 0.79 | 0.04 | 94 | 159 | 0.51 | 0.79 | 0.04 | 80 | 25 | 0.07 | 0.79 | 0.04 | 88 |
| | Ji_Parana_SE | 36 | 0.64 | 1.87 | 0.08 | 61 | 188 | 0.93 | 1.16 | 0.20 | 77 | 54 | 0.92 | 1.19 | 0.33 | 74 |
| | La Paz | 230 | 0.10 | 0.63 | 0.04 | 91 | 291 | 0.50 | 0.31 | 0.08 | 54 | 81 | 0.65 | 0.33 | 0.09 | 53 |
| | Manaus Embrapa | 0 | – | – | – | – | 10 | 0.97 | 1.38 | 0.15 | 40 | 2 | – | – | – | – |
| | Rio Branco | 24 | 0.05 | 1.98 | 0.09 | 46 | 148 | 0.96 | 1.07 | 0.11 | 76 | 54 | 0.96 | 1.10 | 0.13 | 76 |
| | Santa Cruz Utepsa | 108 | 0.65 | 1.17 | 0.06 | 88 | 357 | 0.93 | 0.87 | 0.08 | 76 | 121 | 0.91 | 0.88 | 0.09 | 74 |
| VIIRS DT | Alta Floresta | 89 | 0.29 | 1.25 | 0.17 | 58 | 291 | 0.92 | 1.13 | 0.17 | 59 | 97 | 0.90 | 1.21 | 0.27 | 58 |
| | Amazon ATTO Tower | 34 | 0.84 | 2.33 | 0.12 | 12 | 80 | 0.90 | 1.67 | 0.14 | 18 | 20 | 0.91 | 1.61 | 0.14 | 30 |
| | ARM Manacapuru | 20 | 0.48 | 2.14 | 0.10 | 25 | 48 | 0.93 | 1.26 | 0.14 | 64 | 15 | 0.85 | 1.23 | 0.11 | 60 |
| | Huancayo-IGP | 162 | 0.33 | 0.73 | 0.07 | 52 | 139 | 0.37 | 0.73 | 0.07 | 56 | 20 | 0.13 | 0.73 | 0.07 | 60 |
| | Ji_Parana_SE | 72 | 0.56 | 1.98 | 0.09 | 46 | 231 | 0.95 | 1.21 | 0.24 | 51 | 67 | 0.96 | 1.30 | 0.38 | 57 |
| | La Paz | 281 | 0.37 | 0.93 | 0.05 | 75 | 260 | 0.63 | 0.77 | 0.06 | 76 | 67 | 0.77 | 0.78 | 0.05 | 84 |
| | Manaus Embrapa | 27 | 0.83 | 2.39 | 0.12 | 11 | 74 | 0.92 | 1.54 | 0.16 | 22 | 14 | 0.83 | 1.50 | 0.11 | 36 |
| | Rio Branco | 51 | 0.51 | 1.67 | 0.08 | 43 | 178 | 0.95 | 1.15 | 0.16 | 71 | 67 | 0.95 | 1.12 | 0.24 | 72 |
| | Santa Cruz Utepsa | 119 | 0.77 | 1.08 | 0.06 | 76 | 359 | 0.92 | 0.97 | 0.14 | 66 | 124 | 0.92 | 0.96 | 0.11 | 65 |

aerosols, e.g., smoke. For satellite data, by definition fine mode is obtained by the product of the total AOD and fine mode fraction (FMF), while the coarse mode is computed by the difference between the total AOD and the fine mode (e.g.; Sayer et al., 2019). For VIIRS retrievals, we used AE to determine the dominant size mode, since FMF is not provided in the VIIRS DB land product (Hsu et al., 2019). Typical values of AE $\leq 1$ indicate the dominance of coarse mode aerosol while AE $> 1$ the dominance of fine mode aerosol particles (Eck et al., 1999). However, AE is degenerate in size and modal contribution compared to fine and coarse mode optical depth and should be considered as a qualitative indicator (Reid et al., 1999; Schuster et al., 2006; Sayer et al., 2019; Reid et al., 2022; Su et al., 2023). Besides the limitations, AE is commonly a qualitative parameter related to aerosol particle size and has been employed in several studies to consider the effect of fine particles like FMF (Sayer et al., 2019; Schuster et al., 2006).

Fig. 7a shows the variation of VIIRS DB and DT AOD retrieval bias as a function of AERONET total AOD. For low aerosol loading (AOD<0.2 and AOD<0.4), DB shows a very low negative median bias, practically negligible, while a positive median bias is achieved with increasing aerosol loading, from 0.2 to 0.14. VIIRS DT also shows a negligible negative median bias for low aerosol loading, while for AOD>0.2, a systematic and increasing positive median bias is noted as aerosol increases, from 0.03 to 1.13. These results indicated greater variability and uncertainty with increasing aerosol loading by both VIIRS algorithms, which can lead to inadequate AOD retrievals of extreme events by overestimations related to aerosol properties.

Retrieval uncertainty of VIIRS DB and DT of aerosol loading conditions under background conditions (AODAERONET≤0.2), intermediate (AODAERONET>0.2) and high event (AODAERONET>0.6) is shown in Table 4. In general, VIIRS DB indicates satisfactory accuracy under all aerosol loading scenarios, with the best accuracy under aerosol background with 81% within EE, although with a significative negative deviation (RMB = 0.87) and low correlation (R = 0.46). In contrast, VIIRS DT shows unsatisfactory accuracy (EE<66%) under all aerosol loading scenarios, probably associated with surface reflectance errors. The EE decreases while RMB increases as the aerosol magnitude increases, although indicates low bias under low aerosol loading compared to VIIRS DB.

Additionally, higher accuracy is indicated for all aerosol loading under wet, dry and burning seasons for VIIRS DB, with an increased negative bias under low aerosol loading during the dry and the burning seasons contrary to the wet season, with positive bias prevalence. Accuracy of 100% within EE is exhibited in the wet season under an intermediate scenario (AOD>0.2) but with a low performance by insignificant correlation. For high aerosol events (AOD>0.6), no matchups are retrieved as expected under clean background conditions. On the other hand, VIIRS DT shows satisfactory accuracy in terms of EE only in the peak burning season, with 67% within EE and no bias. Both DB and DT algorithms show bias increases as the aerosol magnitude increases in relation to total AOD in all period, dry and burning seasons (Table 4).

For aerosol-particle size (Table 4), VIIRS DB shows satisfactory accuracy under the coarse and fine mode, including all polluted scenarios. Both algorithms indicate higher accuracy under coarse mode in terms of EE, RMB and RMSE compared to fine mode dominance, although with lower correlations even for all polluted scenarios. In the presence of fine dominant aerosol in VIIRS DB, a larger positive bias is noted compared to coarse mode, except for the burning season, suggesting high absorption in the selected aerosol models. VIIRS DB show the best performance in the dry season, with 89% within EE under coarse mode. In the wet

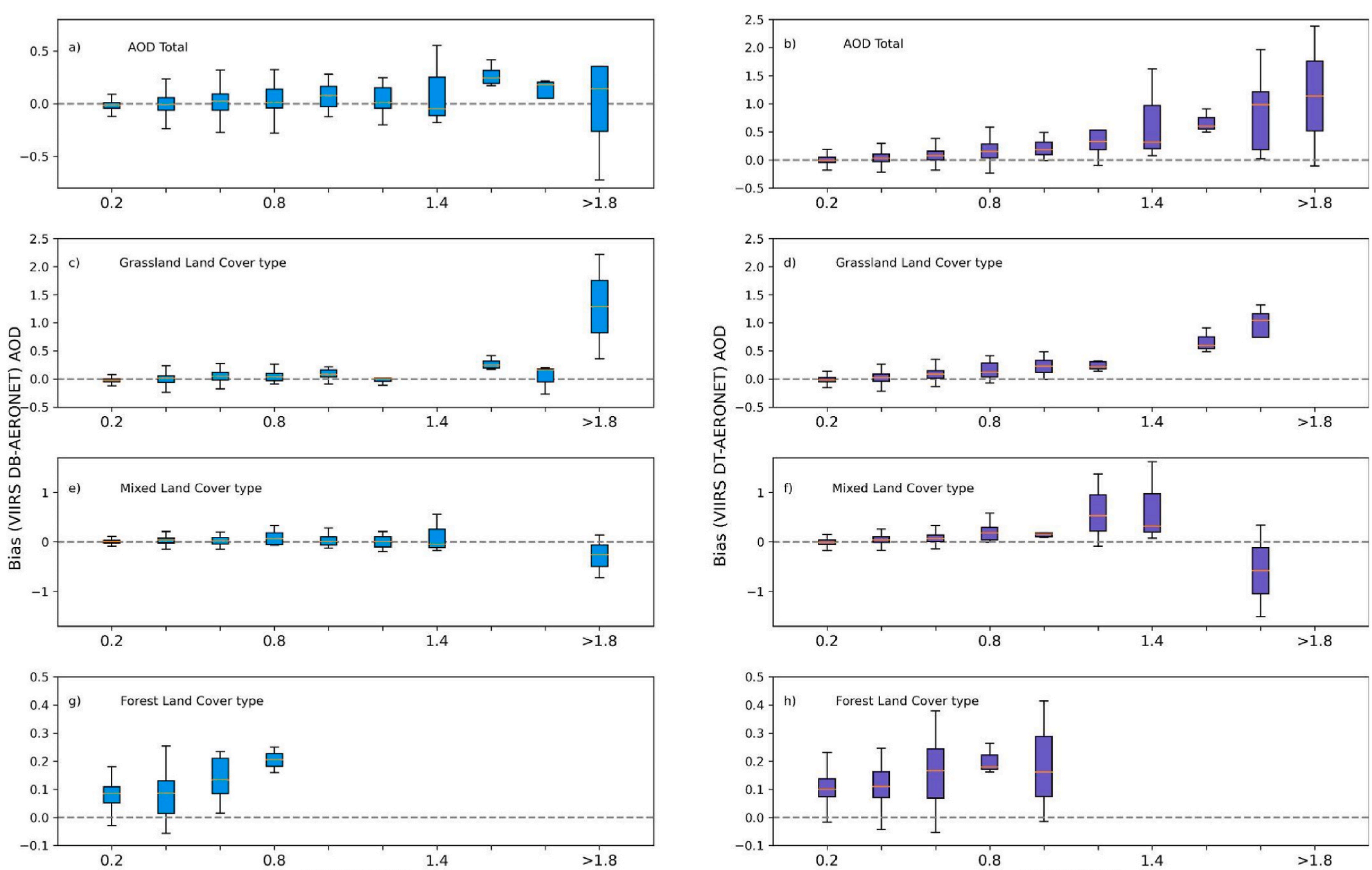


**Fig. 7.** VIIRS DB and DT AOD retrieval bias to loading aerosol for each major land cover type. For each box, the middle line, dot, and upper and lower hinges represent the median, mean, and 25th and 75th percentiles, respectively. The horizontal dashed line represents zero bias.

**Table 4**
Performance of VIIRS DB and DT AOD retrievals according to the dominant aerosol loading and aerosol-particle size based on AERONET AOD-AE.

| Algorithm | Classes | 2012–2022 | | | | | Wet season | | | | | Dry season | | | | | Peak burning season | | | | |
|---|---|---|---|---|---|---|---|---|---|---|---|---|---|---|---|---|---|---|---|---|---|
| | | N | R | RMB | RMSE | EE | N | R | RMB | RMSE | EE | N | R | RMB | RMSE | EE | N | R | RMB | RMSE | EE |
| VIIRS DB | AOD ≤0.2 | 2628 | **0.46** | 0.87 | 0.06 | 81 | 558 | **0.39** | 1.11 | 0.05 | 84 | 856 | **0.54** | 0.77 | 0.06 | 73 | 170 | **0.58** | 0.70 | 0.07 | 73 |
| | AOD >0.2 | 669 | **0.91** | 1.04 | 0.15 | 69 | 7 | 0.62 | 1.07 | 0.05 | 100 | 625 | **0.91** | 1.04 | 0.15 | 69 | 267 | **0.92** | 1.04 | 0.19 | 70 |
| | AOD >0.6 | 84 | **0.87** | 1.08 | 0.29 | 73 | 0 | – | – | – | – | 80 | **0.87** | 1.08 | 0.29 | 74 | 57 | **0.86** | 1.08 | 0.34 | 72 |
| | Coarse | 455 | **0.41** | 1.20 | 0.06 | 85 | 146 | **0.31** | 1.56 | 0.06 | 78 | 104 | **0.64** | 1.04 | 0.06 | 89 | 15 | **0.81** | 1.18 | 0.08 | 87 |
| | Fine | 2410 | **0.92** | 1.27 | 0.10 | 74 | 332 | **0.49** | 1.90 | 0.07 | 72 | 1193 | **0.93** | 1.18 | 0.07 | 71 | 369 | **0.93** | 1.13 | 0.17 | 71 |
| VIIRS DT | AOD ≤0.2 | 3144 | **0.50** | 1.03 | 0.07 | 61 | 843 | **0.43** | 1.39 | 0.07 | 59 | 905 | **0.58** | 0.90 | 0.08 | 60 | 176 | **0.63** | 1.00 | 0.08 | 67 |
| | AOD >0.2 | 826 | **0.89** | 1.18 | 0.21 | 57 | 12 | −0.08 | 0.85 | 0.45 | 50 | 755 | **0.91** | 1.18 | 0.21 | 59 | 315 | **0.93** | 1.19 | 0.26 | 61 |
| | AOD >0.6 | 92 | **0.75** | 1.28 | 0.47 | 46 | 1 | – | – | – | – | 88 | **0.88** | 1.30 | 0.44 | 45 | 50 | **0.86** | 1.29 | 0.43 | 50 |
| | Coarse | 546 | **0.40** | 1.50 | 0.06 | 63 | 218 | **0.30** | 1.79 | 0.06 | 55 | 103 | **0.78** | 1.30 | 0.07 | 66 | 16 | **0.83** | 1.70 | 0.15 | 63 |
| | Fine | 3042 | **0.91** | 1.46 | 0.13 | 55 | 512 | **0.46** | 2.33 | 0.08 | 52 | 1427 | **0.92** | 1.36 | 0.21 | 53 | 436 | **0.93** | 1.32 | 0.21 | 53 |

season, large positive biases from coarse to fine particle distributions are noted (1.56–1.90). In general, VIIRS DT shows a similar response to VIIRS DB, with increased (decreased) bias (EE) from coarse to fine dominance, except for full period and burning season, and non-satisfactory accuracy values with respect to EE.

The results indicate that the aerosol particle size may dominate the AOD errors in different ways in VIIRS DB and DT algorithms. The highest AOD retrieval uncertainty is mainly evident during fine dominating aerosol in both algorithms, with a systematic positive bias in all polluted scenarios. The large biases can be associated with disparate open path measurements (e.g., Falah et al., 2021). Additionally, coarse aerosol dominance represents the smallest number of matchups in the Amazon Basin compared to fine mode since is more common in arid regions, leading to a poor agreement between VIIRS and AERONET by lower correlations.

### 3.4. *Accuracy of VIIRS AOD under land cover types*

Fig. 7c–h shows the variation of VIIRS DB and DT AOD retrieval bias with respect to AERONET total AOD under each major land cover type in the Amazon Basin. For grassland type, both VIIRS DB and DT indicate almost no bias for low aerosol loading values (AOD<0.4), which further overestimates as AOD increases, especially for high aerosol loading (AOD>1.6). For mixed land cover type, VIIRS DB shows a small positive median bias under AOD>0.4 and AOD<1 while underestimated for AOD>1.4. In contrast, VIIRS DT indicates a widespread positive median bias, especially under AOD>0.6, although it shows a strong negative median bias for higher aerosol (1.6<AOD<1.8). For forest land cover type, both products show overall overestimation as increased magnitude aerosol. It is clear that both algorithms are sensitive to estimate surface reflectance. Wang et al. (2023) also showed that VIIRS DB algorithms overestimated over dense vegetation regions, probably associated with the deviation of the land surface reflectance ratios between visible and shortwave infrared bands.

The performance of VIIRS-AERONET matchups under aerosol loading, aerosol-particle size and surface vegetation type is also shown in Tables 5 and 6. For grassland land cover type, VIIRS DB indicates satisfactory accuracy under both aerosol loading scenarios and under the coarse-fine mode, with the best accuracy in terms of EE and lower RMSE under background conditions (AOD≤0.2) and when coarse particle aerosol dominates. However, DB also indicate a systematic negative bias under low aerosol loading and coarse mode follow by low and non-significate correlations, respectively. VIIRS DT shows satisfactory accuracy only under background loading and for coarse mode; however, both also are followed by low correlation values and with strong negative bias under low aerosol. The seasonal performance, VIIRS DB indicates the best accuracy in the wet season under background conditions, with EE = 86% and under coarse dominance, especially in the burning and dry seasons. For VIIRS DT, satisfactory accuracy is achieved in the dry and burning seasons under low loading and coarse mode conditions, with higher values in the peak burning season, 79% and 90% within EE, respectively.

For mixed land cover type, VIIRS DB presents higher accuracy and almost no bias than grassland coverage in relation to aerosol loading conditions in all period but also presents the best performance under low aerosol loading (EE = 85%). On the other hand, VIIRS DT shows satisfactory accuracy only under intermediate aerosol loading with (EE = 66%), with opposite accuracy compared to grassland coverage. In the wet season, DB shows poor performance under coarse and fine dominance, with large biases (RMB=>2). In the dry and burning seasons, a similar response to grassland coverage is achieved, but with better performance under coarse mode with high correlation, 0.81 although with a positive bias, 1.35 compared to grassland cover type values (0.12 and 0.77, respectively). VIIRS DT indicates no satisfactory accuracy in terms of EE in the polluted scenarios.

In general, both algorithms indicate good accuracy in coarse mode

**Table 5**
Performance of VIIRS DB AOD retrievals according to land cover type, aerosol loading and aerosol-particle size based on AERONET AOD-AE. Only results with at least 4 AOD matchups are shown.

| Land Type | Classes | 2012–2022 | | | | | Wet season | | | | | Dry season | | | | | Peak burning season | | | | |
|---|---|---|---|---|---|---|---|---|---|---|---|---|---|---|---|---|---|---|---|---|---|
| | | N | R | RMB | RMSE | EE | N | R | RMB | RMSE | EE | N | R | RMB | RMSE | EE | N | R | RMB | RMSE | EE |
| Grassland | AOD ≤0.2 | 1826 | **0.33** | 0.75 | 0.05 | 81 | 398 | **0.20** | 0.95 | 0.06 | 86 | 545 | **0.45** | 0.62 | 0.07 | 69 | 114 | **0.48** | 0.55 | 0.07 | 68 |
| | AOD >0.2 | 254 | **0.92** | 1.08 | 0.19 | 67 | 0 | – | – | – | – | 241 | **0.92** | 1.08 | 0.19 | 68 | 100 | **0.92** | 1.12 | 0.26 | 69 |
| | Coarse | 362 | 0.08 | 0.97 | 0.05 | 91 | 118 | 0.19 | 1.26 | 0.05 | 90 | 75 | 0.12 | 0.77 | 0.05 | 92 | 12 | 0.08 | 0.70 | 0.03 | 100 |
| | Fine | 1427 | **0.93** | 1.20 | 0.09 | 81 | 217 | **0.27** | 1.71 | 0.05 | 80 | 604 | **0.93** | 1.12 | 0.13 | 76 | 171 | **0.94** | 1.15 | 0.21 | 72 |
| Mixed | AOD ≤0.2 | 736 | **0.52** | 1.03 | 0.06 | 85 | 153 | **0.41** | 1.36 | 0.07 | 79 | 291 | **0.56** | 0.90 | 0.06 | 82 | 49 | **0.56** | 0.85 | 0.06 | 90 |
| | AOD >0.2 | 381 | **0.91** | 1.00 | 0.12 | 72 | 7 | 0.62 | 1.07 | 0.04 | 100 | 355 | **0.91** | 0.99 | 0.12 | 72 | 162 | **0.93** | 0.97 | 0.12 | 71 |
| | Coarse | 81 | **0.66** | 1.85 | 0.07 | 69 | 25 | **0.50** | 2.63 | 0.09 | 32 | 26 | **0.81** | 1.35 | 0.06 | 92 | 2 | – | – | – | – |
| | Fine | 899 | **0.93** | 1.28 | 0.10 | 69 | 111 | **0.55** | 2.08 | 0.09 | 59 | 544 | **0.93** | 1.18 | 0.11 | 70 | 187 | **0.95** | 1.10 | 0.12 | 73 |
| Forest | AOD ≤0.2 | 66 | **0.70** | 1.81 | 0.10 | 35 | 7 | 0.69 | 2.21 | 0.13 | 29 | 20 | 0.68 | 1.69 | 0.12 | 35 | 7 | 0.44 | 1.48 | 0.08 | 43 |
| | AOD >0.2 | 34 | **0.95** | 1.27 | 0.13 | 47 | 0 | – | – | – | – | 29 | **0.95** | 1.27 | 0.13 | 45 | 5 | **0.97** | 1.17 | 0.12 | 40 |
| | Coarse | 12 | **0.63** | 2.16 | 0.14 | 25 | – | **-** | – | – | – | 45 | **0.93** | 1.82 | 0.20 | 11 | 11 | **0.97** | 1.80 | 0.16 | 18 |
| | Fine | 376 | **0.91** | 2.35 | 0.20 | 5 | 40 | **0.30** | 5.03 | 0.13 | 5 | 186 | **0.90** | 2.05 | 0.21 | 6 | 44 | **0.83** | 2.11 | 0.20 | 11 |

**Table 6**
Performance of VIIRS DT AOD retrievals according to land cover type, aerosol loading and aerosol-particle size based on AERONET AOD-AE.

| Land Type | Classes | 2012–2022 | | | | | Wet season | | | | | Dry season | | | | | Peak burning season | | | | |
|---|---|---|---|---|---|---|---|---|---|---|---|---|---|---|---|---|---|---|---|---|---|
| | | N | R | RMB | RMSE | EE | N | R | RMB | RMSE | EE | N | R | RMB | RMSE | EE | N | R | RMB | RMSE | EE |
| Grassland | AOD ≤0.2 | 1997 | **0.45** | 0.88 | 0.06 | 66 | 565 | **0.38** | 1.28 | 0.07 | 62 | 518 | **0.53** | 0.78 | 0.07 | 68 | 99 | **0.65** | 0.87 | 0.06 | 79 |
| | AOD >0.2 | 305 | **0.94** | 1.19 | 0.24 | 58 | 1 | – | – | – | – | 290 | **0.94** | 1.20 | 0.25 | 58 | 122 | **0.95** | 1.26 | 0.33 | 62 |
| | Coarse | 372 | **0.47** | 1.21 | 0.07 | 74 | 483 | **0.20** | 2.50 | 0.09 | 54 | 146 | **0.51** | 1.60 | 0.08 | 66 | 10 | **0.62** | 1.03 | 0.04 | 90 |
| | Fine | 1705 | **0.94** | 1.33 | 0.10 | 63 | 337 | **0.38** | 2.26 | 0.08 | 56 | 682 | **0.95** | 1.26 | 0.14 | 62 | 195 | **0.97** | 1.29 | 0.19 | 62 |
| Mixed | AOD ≤0.2 | 813 | **0.54** | 0.90 | 0.06 | 65 | 199 | **0.50** | 1.25 | 0.06 | 69 | 195 | **0.61** | 0.76 | 0.07 | 59 | 53 | **0.65** | 0.80 | 0.07 | 62 |
| | AOD >0.2 | 385 | **0.85** | 1.11 | 0.21 | 66 | 9 | 0.13 | 0.71 | 0.51 | 56 | 355 | **0.89** | 1.12 | 0.20 | 67 | 168 | **0.89** | 1.12 | 0.22 | 62 |
| | Coarse | 108 | **0.36** | 1.26 | 0.14 | 58 | 43 | **0.36** | 1.40 | 0.20 | 49 | 28 | **0.82** | 0.90 | 0.07 | 57 | 2 | – | – | – | – |
| | Fine | 961 | **0.91** | 1.34 | 0.14 | 61 | 135 | **0.67** | 1.99 | 0.08 | 56 | 559 | **0.91** | 1.29 | 0.18 | 57 | 197 | **0.89** | 1.26 | 0.22 | 54 |
| Forest | AOD ≤0.2 | 334 | **0.69** | 2.05 | 0.12 | 19 | 79 | **0.61** | 2.40 | 0.12 | 16 | 92 | **0.71** | 1.82 | 0.13 | 22 | 24 | **0.67** | 1.80 | 0.14 | 29 |
| | AOD >0.2 | 136 | **0.88** | 1.39 | 0.20 | 32 | 2 | – | – | – | – | 110 | **0.90** | 1.38 | 0.16 | 33 | 52 | **0.88** | 1.27 | 0.12 | 52 |
| | Coarse | 10 | **0.93** | 2.57 | 0.23 | 1 | 29 | **0.83** | 2.94 | 0.16 | 3 | 10 | **0.93** | 2.57 | 0.23 | 1 | 4 | 0.93 | 2.35 | 0.27 | 1 |
| | Fine | 376 | **0.91** | 2.35 | 0.20 | 5 | 40 | **0.30** | 5.03 | 0.13 | 5 | 186 | **0.90** | 2.05 | 0.21 | 6 | 44 | **0.83** | 2.11 | 0.20 | 11 |

compared to fine mode, although for VIIRS DB, uncertainty increases with vegetation characteristics in all pollution scenarios. For grassland, it presents systematic negative biases and no significant correlations, while for mixed land cover, coarse dominance is followed by large biases and low correlation than fine mode. Both VIIRS DB and DT AOD retrievals trends to underestimate (overestimate) under background (intermediate) aerosol conditions over grassland land cover type in all period and polluted scenarios. VIIRS DT also presents the same response to mixed land cover type, except in the wet season, whose biases are inverse to grassland.

The seasonal performance of VIIRS DB shows high variability in relation to biases under mixed coverage, with large positive biases in the wet season contrasting with negative biases in the dry and burning seasons. VIIRS DB also underestimates (overestimates) under coarse (fine) mode over grassland land cover type in the full period and polluted scenarios, except in the wet season with large positive biases (1.26 and 1.71, respectively). VIIRS DT also exhibits a large positive bias, especially for coarse mode under grassland. Payra et al. (2023) noticed that VIIRS AOD overestimates coarse-mode particles over bright surfaces like deserts due to scattering and absorbing light efficiency. For mixed land cover, DT shows negative bias only in the dry season under coarse dominance.

For forest land cover type, poor accuracy is indicated for VIIRS DB and DT AOD retrievals followed by a large positive bias (between 1.39 and 2.57), higher RMSE (0.10–0.23), although with a higher correlation compared to grassland and mixed surface coverage for almost all classes, considering the full period 2012–2022. A large positive bias is also indicated in the seasonal performance for both algorithms. Wang et al. (2020) also indicated poor accuracy of VIIRS AOD retrievals over forest land cover and better accuracy under grassland in Asia. Aditi et al. (2023) showed that VIIRS DB retrieval accuracy declined with increased vegetation coverage. A widespread overestimation is noted by both VIIRS algorithms with respect to aerosol loading and particle sizes under forest land cover in all seasons. This widespread overestimate is also noted in the wet season with respect to all land cover types probably associated with decreased surface reflectance due to the amount of water vapor available in the atmosphere (e.g., Payra et al., 2023).

## 4. Conclusions

This study evaluates the performance and accuracy of VIIRS DB and DT AOD retrievals over the Amazon Basin under distinct air pollution scenarios using AERONET measurements. VIIRS-AERONET matchups in site-scale performance and retrieval algorithm uncertainty were also comprehensively evaluated under varying aerosol loading, particle size distribution and surface land cover types.

The overall performance showed that the VIIRS DB algorithm indicated high accuracy in terms of the AOD retrievals within the one-standard-deviation-confidence interval of AERONET AOD, with 78% of matchups falling within the expected error, 84% in the wet season and 71% in the dry and peak burning seasons. In contrast, VIIRS DT showed low accuracy in terms of retrievals falling within the EE, with 64% within EE, 63% in the wet season, 61% in the dry season and 64% in the peak burning seasons. In general, VIIRS DB total AOD retrievals slightly underestimated the AERONET measurements, except in the wet season, while VIIRS DT overestimated AOD in full period, clean and polluted scenarios.

Regionally, VIIRS DB AOD retrievals performed best in six of the nine AERONET sites in the Amazon Basin, varying between 72% and 91% within the expected error level. VIIRS DT showed satisfactory accuracy in four sites, with 66%–81% within EE. Our results demonstrated that both VIIRS algorithms were unable to satisfactorily retrieve AOD over AERONET sites with densely vegetated surfaces as forest land cover types and under high elevations.

VIIRS DB trends to underestimated aerosol under background conditions and showed an increased positive deviation from coarse to fine mode. Both VIIRS DB and DT systematically overestimated AERONET AOD as increased aerosol loading. VIIRS DT presented systematically larger biases than VIIRS DB, especially under coarse and fine mode. In terms of accuracy, DB showed satisfactory values within EE for both aerosol loading (EE>69%) and aerosol particle sizes (EE>71%), while DT showed satisfactory accuracy just under aerosol background conditions in the peak burning season (EE = 67%) and under coarse dominance in the dry season (E = 66%).

Retrieval accuracy of both VIIRS DB and DT algorithms indicated poor accuracy under forest land cover type, with large positive bias in all air polluted scenarios. In general, VIIRS DB performed better under aerosol loading for mixed land cover type and under coarse and fine distributions for grassland coverage. VIIRS DT indicated satisfactory accuracy only under low aerosol loading and coarse dominance for grassland, with best performance in the peak of burning while for mixed coverage only under intermediate aerosol loading. Both algorithms show greater uncertainty associated with the coarse particle aerosol for the full period and all polluted scenarios. DB systematically indicates negative biases under coarse mode followed by very low and non-significant correlations under grassland coverage, while for mixed land cover type, large positive bias and low correlation than fine mode dominance.

These results indicate that the VIIRS AOD algorithm needs improved retrievals over the Amazon Basin, especially under high-elevation, particle size aerosol and vegetated surface coverage. However, it is essential to conduct further in-depth investigations into the causes of the pointed errors and uncertainties found. Results also may contribute to aerosol-related studies, especially in regions without continuous monitoring and sparse coverage of ground-based stations, such as the Amazon Basin. The continuity and installation of AERONET sites with better coverage over the Amazon are essential to improve aerosol climate studies and validations since satellite AOD retrievals in some locations are less accurate, leading to more significant uncertainties.

## CRediT authorship contribution statement

**Vanúcia Schumacher:** Conceptualization, Data curation, Formal analysis, Investigation, Methodology, Validation, Writing – original draft. **Alberto Setzer:** Conceptualization, Project administration, Supervision, Writing – review & editing.

## Declaration of competing interest

The authors declare that they have no known competing financial interests or personal relationships that could have appeared to influence the work reported in this paper.

## Data availability

Data will be made available on request.

## Acknowledgments

This study was supported by funding from the São Paulo Research Foundation - FAPESP (grant no. 2022/01829-8). We gratefully acknowledge the support of the RCGI – Research Centre for Greenhouse Gas Innovation (January 23, 8493.1.9), hosted by the University of São Paulo (USP) and sponsored by FAPESP (2020/15230-5) and Shell Brasil, as well as the strategic importance of the support given by ANP (Brazil's National Oil, Natural Gas and Biofuels Agency) through the R&DI levy regulation. We also thank P.S.S. Victorino's support in data coding.

## References


Aditi, K., Singh, A., Banerjee, T., 2023. Retrieval Uncertainty and Consistency of Suomi-NPP VIIRS Deep Blue and Dark Target Aerosol Products under Diverse Aerosol Loading Scenarios over South Asia. Environmental Pollution, 121913.

Arias, M.E., Farinosi, F., Lee, E., Livino, A., Briscoe, J., Moorcroft, P.R., 2020. Impacts of climate change and deforestation on hydropower planning in the Brazilian Amazon. Nat. Sustain. 3 (6), 430–436.

Bellouin, N., Quaas, J., Gryspeerdt, E., Kinne, S., Stier, P., Watson-Parris, D., et al., 2020. Bounding global aerosol radiative forcing of climate change. Rev. Geophys. 58 (1), e2019RG000660.

Butt, E.W., Rap, A., Schmidt, A., Scott, C.E., Pringle, K.J., Reddington, C.L., et al., 2016. The impact of residential combustion emissions on atmospheric aerosol, human health, and climate. Atmos. Chem. Phys. 16 (2), 873–905.

Chen, Q.X., Han, X.L., Gu, Y., Yuan, Y., Jiang, J.H., Yang, X.B., et al., 2022. Evaluation of MODIS, MISR, and VIIRS daily level-3 aerosol optical depth products over land. Atmos. Res. 265, 105810.

Chu, D.A., Kaufman, Y.J., Ichoku, C., Remer, L.A., Tanré, D., Holben, B.N., 2002. Validation of MODIS aerosol optical depth retrieval over land. Geophys. Res. Lett. 29 (12). MOD2-1.

Davidson, E.A., de Araújo, A.C., Artaxo, P., Balch, J.K., Brown, I.F., C.Bustamante, M.M., et al., 2012. The Amazon basin in transition. Nature 481 (7381), 321–328.

Eck, T.F., Holben, B.N., Reid, J.S., Dubovik, O., Smirnov, A., O'neill, N.T., et al., 1999. Wavelength dependence of the optical depth of biomass burning, urban, and desert dust aerosols. J. Geophys. Res. Atmos. 104 (D24), 31333–31349.

Eufemia, L., Dias Turetta, A.P., Bonatti, M., Da Ponte, E., Sieber, S., 2022. Fires in the Amazon region: quick policy review. Dev. Pol. Rev. 40 (5), e12620.

Falah, S., Mhawish, A., Sorek-Hamer, M., Lyapustin, A.I., Kloog, I., Banerjee, T., et al., 2021. Impact of environmental attributes on the uncertainty in MAIAC/MODIS AOD retrievals: a comparative analysis. Atmos. Environ. 262, 118659.

Fan, R., Ma, Y., Jin, S., Gong, W., Liu, B., Wang, W., et al., 2023. Validation, analysis, and comparison of MISR V23 aerosol optical depth products with MODIS and AERONET observations. Sci. Total Environ. 856, 159117.

Giles, D.M., Sinyuk, A., Sorokin, M.G., Schafer, J.S., Smirnov, A., Slutsker, I., et al., 2019. Advancements in the Aerosol Robotic Network (AERONET) Version 3 database–automated near-real-time quality control algorithm with improved cloud screening for Sun photometer aerosol optical depth (AOD) measurements. Atmos. Meas. Tech. 12 (1), 169–209.

Gui, K., Che, H., Wang, Y., Xia, X., Holben, B.N., Goloub, P., et al., 2021. A global-scale analysis of the MISR Level-3 aerosol optical depth (AOD) product: comparison with multi-platform AOD data sources. Atmos. Pollut. Res. 12 (12), 101238.

Gumber, A., Reid, J.S., Holz, R.E., Eck, T.F., Hsu, N.C., Levy, R.C., et al., 2022. Assessment of severe aerosol events from NASA MODIS and VIIRS aerosol products for data assimilation and climate continuity. Atmospheric Measur. Tech. Discuss. 2022, 1–46.

He, L., Wang, L., Li, Z., Jiang, D., Sun, L., Liu, D., et al., 2021. VIIRS environmental data record and deep blue aerosol products: validation, comparison, and spatiotemporal variations from 2013 to 2018 in China. Atmos. Environ. 250, 118265.

Holben, B.N., Eck, T.F., Slutsker, I., Tanré, D., Buis, J.P., Setzer, A., et al., 1998. AERONET—a federated instrument network and data archive for aerosol characterization. Rem. Sens. Environ. 66 (1), 1–16. https://doi.org/10.1016/S0034-4257(98)00031-5.

Hsu, N.C., Lee, J., Sayer, A.M., Kim, W., Bettenhausen, C., Tsay, S.C., 2019. VIIRS Deep Blue aerosol products over land: extending the EOS long-term aerosol data records. J. Geophys. Res. Atmos. 124 (7), 4026–4053.

Huang, F., Ma, W., Wang, S., Feng, C., Kong, X., Liu, H., 2023. Analysis and validation of the aerosol optical depth of MODIS products in Gansu Province, Northwest China. Rem. Sens. 15 (12), 2972.

Ichoku, C., Chu, D.A., Mattoo, S., Kaufman, Y.J., Remer, L.A., Tanré, D., et al., 2002. A spatio-temporal approach for global validation and analysis of MODIS aerosol products. MOD1-1 Geophys. Res. Lett. 29 (12).

Ignotti, E., Valente, J.G., Longo, K.M., Freitas, S.R., Hacon, S.D.S., Artaxo Netto, P., 2010. Impact on human health of particulate matter emitted from burnings in the Brazilian Amazon region. Rev. Saude Publica 44, 121–130.

IPCC, 2021. Intergovernmental Panel on Climate Change, AR6 Climate Change 2021: the Physical Science Basis. Jia, Z., Lin, B., 2021.

Jiang, D., Wang, L., Yi, X., Su, X., Zhang, M., 2022. Comprehensive evaluation of multisource aerosol optical depth gridded products over China. Atmos. Environ. 278, 119088.

Karra, K., Kontgis, C., Statman-Weil, Z., Mazzariello, J.C., Mathis, M., Brumby, S.P., 2021. Global land use/land cover with Sentinel 2 and deep learning. In: 2021 IEEE International Geoscience and Remote Sensing Symposium IGARSS. IEEE, pp. 4704–4707.

Kok, J.F., Storelvmo, T., Karydis, V.A., Adebiyi, A.A., Mahowald, N.M., Evan, A.T., et al., 2023. Mineral dust aerosol impacts on global climate and climate change. Nat. Rev. Earth Environ. 4 (2), 71–86.

Lapola, D.M., Pinho, P., Barlow, J., Aragão, L.E., Berenguer, E., Carmenta, R., et al., 2023. The drivers and impacts of Amazon forest degradation. Science 379 (6630), eabp8622.

Levy, R., Hsu, C., et al., 2015. MODIS atmosphere L2 aerosol product. In: NASA MODIS Adaptive Processing System. Goddard Space Flight Center, USA. https://doi.org/10.5067/MODIS/MYD04_L2.061.

Lima, A., Silva, T.S.F., de Feitas, R.M., Adami, M., Formaggio, A.R., Shimabukuro, Y.E., 2012. Land use and land cover changes determine the spatial relationship between fire and deforestation in the Brazilian Amazon. Appl. Geogr. 34, 239–246.

Llopart, M., Reboita, M.S., Coppola, E., Giorgi, F., Da Rocha, R.P., De Souza, D.O., 2018. Land use change over the Amazon Forest and its impact on the local climate. Water 10 (2), 149.

Lovejoy, T.E., Nobre, C., 2019. Amazon tipping point: last chance for action. Sci. Adv. 5 (12), eaba2949.

Martonchik, J.V., Diner, D.J., Kahn, R., Gaitley, B., Holben, B.N., 2004. Comparison of MISR and AERONET aerosol optical depths over desert sites. Geophys. Res. Lett. 31 (16).

Montalván-Burbano, N., Velastegui-Montoya, A., Gurumendi-Noriega, M., Morante-Carballo, F., Adami, M., 2021. Worldwide research on land use and land cover in the amazon region. Sustainability 13 (11), 6039.

Morello, T.F., 2023. Hospitalization due to fire-induced pollution in the Brazilian Amazon: a causal inference analysis with an assessment of policy trade-offs. World Dev. 161, 106123.

Mushtaq, Z., Sharma, M., Bangotra, P., Gautam, A.S., Gautam, S., 2022. Atmospheric aerosols: some highlights and highlighters, past to recent years. Aerosol Sci. Eng. 6 (2), 135–145.

O'Neill, N.T., Eck, T.F., Smirnov, A., Holben, B.N., Thulasiraman, S., 2003. Spectral discrimination of coarse and fine mode optical depth. J. Geophys. Res. 108, 4559–4573.

O'Neill, N.T., Dubovik, O., Eck, T.F., 2001. Modified Ångström exponent for the characterization of submicrometer aerosols. Appl. Opt. 40, 2368–2375.

O'Neill, N., Eck, T., Smirnov, A., Holben, B., Thulasiraman, S., 2006. Spectral Deconvolution Algorithm Technical Memo (Tech. rep.). Green-belt, MD. revision April 26, 2006, version 4 available online from:. NASAGoddard Space Flight Center http://aeronet.gsfc.nasa.gov/new_web/PDF/tauf_tauc_technical_memo1.pdf. December 2023.

Palácios, R., Nassarden, D.C., Franco, M.A., Morais, F.G., Machado, L.A., Rizzo, L.V., et al., 2022. Evaluation of MODIS dark target AOD product with 3 and 10 km resolution in amazonia. Atmosphere 13 (11), 1742.

Payra, S., Sharma, A., Mishra, M.K., Verma, S., 2023. Performance evaluation of MODIS and VIIRS satellite AOD products over the Indian subcontinent. Front. Environ. Sci. 11, 1158641.

Peng, J., Yu, P., Yu, Y., Jia, A., Wang, D., Wang, H., Wang, Z., 2023. An evaluation of the NOAA global daily gap-filled VIIRS surface albedo. Rem. Sens. Environ. 298, 113822.

Petrenko, C.L., Friend, A., Garrido, E.F., Taussig, H.N., Culhane, S.E., 2012. Does subtype matter? Assessing the effects of maltreatment on functioning in preadolescent youth in out-of-home care. Child Abuse Neglect 36 (9), 633–644.

Pires, J.M., 1984. The amazonian forest. In: The Amazon: Limnology and Landscape Ecology of a Mighty Tropical River and its Basin. Springer Netherlands, Dordrecht, pp. 581–602.

Prist, P.R., Sangermano, F., Bailey, A., Bugni, V., Villalobos-Segura, M.D.C., Pimiento-Quiroga, N., et al., 2023. Protecting Brazilian Amazon Indigenous territories reduces atmospheric particulates and avoids associated health impacts and costs. Commun. Earth Environ. 4 (1), 34.

Qin, W., Fang, H., Wang, L., Wei, J., Zhang, M., Su, X., et al., 2021. MODIS high-resolution MAIAC aerosol product: global validation and analysis. Atmos. Environ. 264, 118684.

Ren-Jian, Z., Kin-Fai, H.O., Zhen-Xing, S., 2012. The role of aerosol in climate change, the environment, and human health. Atmospheric Oceanic Sci. Lett. 5 (2), 156–161.

Rocha, R., Sant'Anna, A.A., 2022. Winds of fire and smoke: air pollution and health in the Brazilian Amazon. World Dev. 151, 105722.

Rogozovsky, I., Ohneiser, K., Lyapustin, A., Ansmann, A., Chudnovsky, A., 2023. The Impact of Different Aerosol Layering Conditions on the High-Resolution MODIS/MAIAC AOD Retrieval Bias: the Uncertainty Analysis. Atmospheric Environment, 119930.

Ruiz-Vásquez, M., Arias, P.A., Martínez, J.A., Espinoza, J.C., 2020. Effects of Amazon basin deforestation on regional atmospheric circulation and water vapor transport towards tropical South America. Clim. Dynam. 54, 4169–4189.

Sawyer, V., Levy, R.C., Mattoo, S., Cureton, G., Shi, Y., Remer, L.A., 2020. Continuing the MODIS dark target aerosol time series with VIIRS. Rem. Sens. 12 (2), 308.

Sayer, A.M., Hsu, N.C., Bettenhausen, C., Jeong, M.J., 2013. Validation and uncertainty estimates for MODIS Collection 6 "Deep Blue" aerosol data. J. Geophys. Res. Atmos. 118 (14), 7864–7872.

Sayer, A.M., Munchak, L.A., Hsu, N.C., Levy, R.C., Bettenhausen, C., Jeong, M.J., 2014. MODIS Collection 6 aerosol products: comparison between Aqua's e-Deep Blue, Dark Target, and "merged" data sets, and usage recommendations. J. Geophys. Res. Atmos. 119 (24), 13–965.

Sayer, A.M., Hsu, N.C., Lee, J., Kim, W.V., Dutcher, S.T., 2019. Validation, stability, and consistency of MODIS collection 6.1 and VIIRS version 1 deep blue aerosol data over land. J. Geophys. Res. Atmos. 124, 4658–4688.

Schuster, G.L., Dubovik, O., Holben, B.N., 2006. Angstrom exponent and bimodal aerosol size distributions. J. Geophys. Res. Atmos. 111 (D7).

Su, Y., Xie, Y., Tao, Z., Hu, Q., Yu, T., Gu, X., 2021. Validation and inter-comparison of MODIS and VIIRS aerosol optical depth products against data from multiple observation networks over East China. Atmos. Environ. 247, 118205.

Su, X., Wei, Y., Wang, L., Zhang, M., Jiang, D., Feng, L., 2022. Accuracy, stability, and continuity of AVHRR, SeaWiFS, MODIS, and VIIRS deep blue long-term land aerosol retrieval in Asia. Sci. Total Environ. 832, 155048.

Su, X., Cao, M., Wang, L., Gui, X., Zhang, M., Huang, Y., Zhao, Y., 2023. Validation, inter-comparison, and usage recommendation of six latest VIIRS and MODIS aerosol products over the ocean and land on the global and regional scales. Sci. Total Environ. 884, 163794.

Wang, Y., Yuan, Q., Shen, H., Zheng, L., Zhang, L., 2020. Investigating multiple aerosol optical depth products from MODIS and VIIRS over Asia: evaluation, comparison, and merging. Atmos. Environ. 230, 117548.

Wang, P., Tang, Q., Zhu, Y., Zheng, K., Liang, T., Yu, Q., He, Y., 2022. Validation and analysis of MAIAC AOD aerosol products in East Asia from 2011 to 2020. Rem. Sens. 14 (22), 5735.
Wang, Q., Li, S., Yang, J., Zhou, D., 2023. Evaluation and comparison of VIIRS dark target and deep blue aerosol products over land. Sci. Total Environ. 869, 161667.
Wei, J., Peng, Y., Guo, J., Sun, L., 2019a. Performance of MODIS Collection 6.1 Level 3 aerosol products in spatial-temporal variations over land. Atmos. Environ. 206, 30–44.
Wei, J., Li, Z., Peng, Y., Sun, L., 2019b. MODIS Collection 6.1 aerosol optical depth products over land and ocean: validation and comparison. Atmos. Environ. 201, 428–440.
Xu, X., Zhang, X., Riley, W.J., Xue, Y., Nobre, C.A., Lovejoy, T.E., Jia, G., 2022. Deforestation triggering irreversible transition in Amazon hydrological cycle. Environ. Res. Lett. 17 (3), 034037.